Activity-evoked and spontaneous opening of synaptic fusion pores

Dinara Bulgari[a], David L. Deitcher[b], Brigitte F. Schmidt[c], M. Alexandra Carpenter[d], Christopher Szent-Gyorgyi[c], Marcel P. Bruchez[c,d,e], and Edwin S. Levitan[a,1]

[a]Department of Pharmacology and Chemical Biology, University of Pittsburgh, Pittsburgh, PA 15261; [b]Department of Neurobiology and Behavior, Cornell University, Ithaca, NY 14853; [c]Molecular Biosensor and Imaging Center, Carnegie Mellon University, Pittsburgh, PA 15213; [d]Department of Chemistry, Carnegie Mellon University, Pittsburgh, PA 15213; and [e]Department of Biological Sciences, Carnegie Mellon University, Pittsburgh, PA 15213

Edited by Ehud Y. Isacoff, University of California, Berkeley, CA, and approved July 11, 2019 (received for review March 27, 2019)

Synaptic release of neuropeptides packaged in dense-core vesicles (DCVs) regulates synapses, circuits, and behaviors including feeding, sleeping, and pain perception. Here, synaptic DCV fusion pore openings are imaged without interference from cotransmitting small synaptic vesicles (SSVs) with the use of a fluorogen-activating protein (FAP). Activity-evoked kiss and run exocytosis opens synaptic DCV fusion pores away from active zones that readily conduct molecules larger than most native neuropeptides (i.e., molecular weight [MW] up to, at least, 4.5 kDa). Remarkably, these synaptic fusion pores also open spontaneously in the absence of stimulation and extracellular Ca^{2+}. SNARE perturbations demonstrate different mechanisms for activity-evoked and spontaneous fusion pore openings with the latter sharing features of spontaneous small molecule transmitter release by active zone-associated SSVs. Fusion pore opening at resting synapses provides a mechanism for activity-independent peptidergic transmission.

neuropeptide release | secretory granule | fusion pore | neuromuscular junction | *Drosophila*

Exocytosis of dense-core vesicles (DCVs) has been avidly studied in nonneuronal cells but not in native synapses where neuropeptide release can influence circuits and behavior (1–3). Presynaptic DCVs differ from their nonneuronal counterparts in many respects. For example, they are smaller (~100 nm instead of 300–1,000 nm) (4), allowing them to fit in thin axons and small boutons. Therefore, they cannot form the very large fusion pores produced by neuroendocrine secretory granules (5). GFP-tagged neuropeptide release from newly arriving and docked single DCVs at the *Drosophila* neuromuscular junction (NMJ) type Ib boutons is slow, dynamin dependent, and incomplete, which is suggestive of kiss and run exocytosis without full collapse (6). However, fusion pore gating properties and permeability for molecules the size of neuropeptides (e.g., 0.65–2 kDa for the *Drosophila* NMJ neuropeptides proctolin, myoinhibitory peptide, and crustacean cardioactive peptide) remain unknown.

Fusion pore opening can be detected by imaging extracellular fluorescent dyes entering docked vesicles, but this approach would label both DCVs and small synaptic vesicles (SSVs), which undergo exocytosis–endocytosis cycling to mediate small molecule cotransmission. Here, we selectively image DCV fusion pores by genetically tagging neuronal DCVs with a proneuropeptide fused to a fluorogen-activating protein (FAP). Specifically, we used an antibody-derived light chain variable domain whose fused homodimer (an atypical scFv) binds malachite green (MG) with picomolar affinity to generate far red fluorescence (7, 8). Therefore, applying a variety of membrane impermeant MG derivatives allowed us to image when and where fusion pores open at synapses and to probe their conduction properties. We report that synaptic DCV fusion pores readily conduct molecules that vary in structure, charge, and molecular weight (MW) reaching 4.5 kDa. Most surprising, even though DCVs (unlike SSVs) do not utilize active zones, synaptic DCV fusion pores open spontaneously by a mechanism reminiscent of spontaneous transmission mediated by SSVs.

Results and Discussion

The L5** FAP monomer (8) was cloned into the C-peptide of *Drosophila* insulinlike peptide 2 to make Dilp2-FAP (Fig. 1*A*). Expression of the construct was then induced in *Drosophila* type Is motor neurons. Previously, dimeric FAP constructs have been used because ternary complex formation between the dye and the two variable domain monomers is inefficient at submicromolar concentrations. However, L5** monomers may homodimerize in the absence of an MG ligand with $K_d > 200$ μM (8), a concentration that is far exceeded by neuropeptides in DCVs, and dimerization would be further aided by the self-association of proneuropeptides that promotes packaging in DCVs (9). Although higher order Dilp2-FAP complexes might not readily permeate through the fusion pore, the design of Dilp2-FAP ensured that it would report passage of extracellularly applied membrane impermeant MG derivatives through the fusion pore into the DCV lumen where we reasoned FAP dimers would be present to produce fluorescence (Fig. 1*B*).

At transgenic *Drosophila* NMJs expressing Dilp2-FAP, addition of membrane impermeant MG derivatives (at 300 nM), such as MG-2p (8) and MG-B-Tau (10) (MW of 704 and 1015, respectively, *SI Appendix*, Fig. S1) immediately produced dim spots of fluorescence around type Is boutons, which presumably reports previously secreted Dilp2-FAP. More importantly, upon 10–70 Hz stimulation, boutons became brightly fluorescent (Movie S1). The dramatic increase in signal became evident within seconds in the form of additional small puncta (Fig. 2 *A* and *B*) at an initial rate of 0.43 ± 0.06 s^{-1} (measured per bouton in the first 10 s of stimulation, $n = 23$ boutons from 6 experiments). With continued stimulation of various intensities, the signal grew until individual

Significance

Neuropeptides are released at synapses to regulate mood and behaviors. Using an imaging approach, formation of neuropeptide-conductive fusion pores are detected at intact native synapses. Surprisingly, it is discovered that these fusion pores open occasionally even when the synapse is not electrically active. These spontaneous events are mechanistically different from the fusion pore opening that is evoked typically by bursts of activity. Spontaneous opening of fusion pores constitutes a mechanism for basal synaptic transmission by neuropeptides even when synapses are electrically silent.

Author contributions: D.B., D.L.D., C.S.-G., M.P.B., and E.S.L. designed research; D.B., D.L.D., and E.S.L. performed research; D.L.D., B.F.S., and M.A.C. contributed new reagents/analytic tools; D.B. analyzed data; and E.S.L. wrote the paper.

The authors declare no conflict of interest.

This article is a PNAS Direct Submission.

[1]To whom correspondence may be addressed. Email: elevitan@pitt.edu.

This article contains supporting information online at www.pnas.org/lookup/suppl/doi:10.1073/pnas.1905322116/-/DCSupplemental.

Published online August 5, 2019.

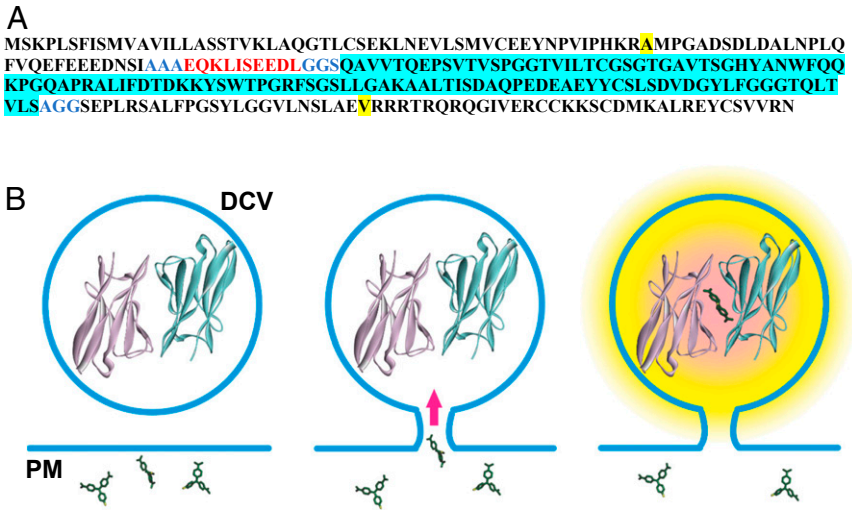

Fig. 1. Design of Dilp2-FAP. (*A*) Amino acid sequence of Dilp2-FAP. Dilp2 sequence is shown in plain black with the beginning and end of the C-peptide (from uniprot.org) highlighted in yellow. The c-Myc tag is red, linker sequences (AAA, GGS, and AGG) are blue, and the FAP monomer inserted in the C-peptide is black with blue highlighting. (*B*) Schematic of FAP experiments. *Left*, fusion with Dilp2 ensures that FAP will be highly concentrated in DCVs so that dimerization can occur (structure from 8). Extracellular MG molecules are shown at different orientations. *Center*, formation of a fusion pore with the plasma membrane (PM) allows extracellular membrane impermeant MG derivatives to enter the DCV lumen. *Right*, formation of complex between the nonfluorescent FAP dimer and MG derivative produces fluorescence. Note that small MG derivatives will diffuse through the fusion pore to increase fluorescence more quickly than exit of large MG-liganded FAP dimers and higher order MG-liganded Dilp2-FAP complexes.

puncta could not be resolved, and the response stopped increasing upon cessation of activity, implying that the response time course was not slowed by the binding kinetics of MG to the FAP. Interestingly, at early stages of the response, individual puncta grew in brightness (Fig. 2*C*), which might reflect multiple DCV fusions at hot spots or compound exocytosis. As expected for DCVs (9), puncta formed away from active zones (the sites of SSV exocytosis) localized based on the ELKS/cytomatrix at the active zone-associated structural protein Bruchpilot (BRP) (Fig. 2*D*). To test if the FAP signal was derived from SNARE-dependent exocytosis, we examined the effect of transgenic expression of the light chain of tetanus toxin (TeTx), a protease that cleaves the *Drosophila* SNARE protein neuronal synaptobrevin (nSyb) (11) to mimic the effect of a null mutant in *Drosophila* and knockout of Syb1 and Syb2 in mice (12, 13). TeTx inhibited Dilp2-FAP responses (Fig. 2 *E* and *F*). Likewise, evoked loss of Dilp2-GFP was also inhibited by TeTx (Fig. 2 *G*–*I*). Thus, the activity-dependent DCV-derived FAP signal relies on the SNARE machinery responsible for neuropeptide release. Finally, consistent with DCV exocytosis, evoked FAP responses could be detected when Ca^{2+} was replaced with Ba^{2+} (Fig. 2*J*).

Two lines of experimentation demonstrated that the observed MG-induced puncta result from labeling of the DCV lumen via the fusion pore. First, a series of MG derivatives (7, 10, 14) was tested each at a concentration of 300 nM. Despite variations in structure, charge, and size (MW 704–4478 Da, *SI Appendix*, Fig. S1), MG derivatives, including a biotin-containing compound (MG-12p-biotin, MW 1327), gave qualitatively similar results (i.e., robust activity-evoked labeling) (Fig. 3 *A*–*C*). However, following conjugation of MG-12p-biotin to streptavidin, application of the ∼55 kDa conjugate (made with two MGs for each streptavidin tetramer to yield 300 nM MG) produced some extracellular labeling initially, but there was no marked response to activity (Fig. 3 *D*, second panel). Strikingly, subsequent stimulation after replacing the conjugate with MG-B-Tau gave robust activity-evoked labeling, showing that the preparation was alive and functional (Fig. 3 *D*, last panel). The initial activity-independent labeling shows that the biotin-MG/streptavidin conjugate interacts with accessible previously released extracellular FAP. Furthermore, the failure to increase conjugate labeling with activity is accounted for by the conjugate being too large to pass through synaptic fusion pores, which are then evident with the free MG derivative. Therefore, these data suggest that the signal produced by free MG derivatives is from passage of <4.5 kDa molecules through the fusion pore to label the neuropeptide-FAP construct inside DCVs.

This conclusion was independently verified by the observation that MG-2p puncta could move inside boutons and translocate into the axon to undergo retrograde transport (Movies S2 and S3). Consistent with the prior finding of DCVs moving from boutons into the axon (15), FAP labeling in the axon colocalized with Dilp2-GFP (Fig. 3*E*). These results show independently that DCVs inside the neuron were labeled by extracellular permeation of a MG derivative through the fusion pore that forms during kiss and run exocytosis. Because these DCV fusion pores conduct a variety of molecules with MWs reaching 4478 Da, they must be permeable to the smaller neuropeptides expressed in type Is motor neurons, such as proctolin (MW 649 Da) (16, 17). Thus, FAP imaging reinforces the conclusion that activity-dependent peptidergic neurotransmission is mediated by fusion pores that form transiently by kiss and run exocytosis (i.e., without full collapse of the DCV).

Unexpectedly, FAP experiments revealed an occasional fusion pore opening before initiating stimulation. To determine if this was due to Ca^{2+} influx, experiments were performed in the absence of extracellular Ca^{2+} and the presence of the Ca^{2+} chelator EGTA. As noted above, immediately after MG-2p application some labeling was evident, which likely reflected previously released FAP. However, over a period of many minutes, new puncta appeared despite the absence of Ca^{2+} influx (Fig. 4 *A* and *B* and Movie S4), resulting in a slow overall increase (Fig. 4 *C* and *D*). Quantification showed that the spontaneous rate was ∼1% of the rate in the first 10 s of stimulation. Furthermore, the spontaneous rate (measured per bouton) was unaffected by MG derivative size (MW 704: 0.32 ± 0.04 min^{-1}, $n = 10$ versus MW 4478: 0.36 ± 0.06 min^{-1}, $n = 5$) or the presence of extracellular Ca^{2+} (see below). As noted with activity responses, labeled puncta could leave boutons to enter the axon, and bright puncta did not appear spontaneously with streptavidin-MG conjugates. Experiments also established that spontaneous DCV exocytosis, such as activity-evoked responses, does not occur at active zones.

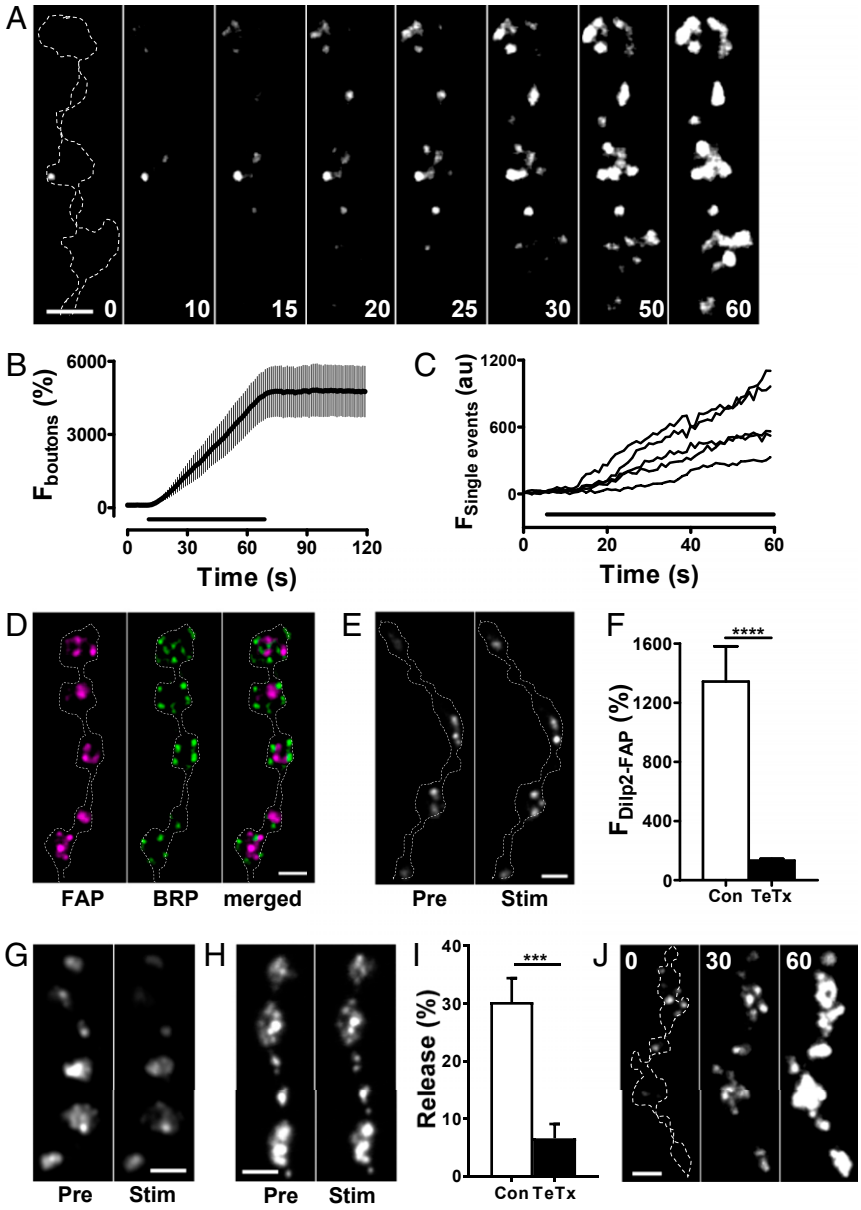

Fig. 2. Activity induces opening of DCV fusion pores in synaptic boutons. (*A*) Contrast-enhanced fluorescent mages of Dilp2-FAP expressing type Is boutons during 30 Hz stimulation for 60 s in the presence of MG-2p. Outline of boutons shown by the dashed line in the first panel. Numbers on the images indicate stimulation time in seconds. A low pass Gaussian blur filter was applied to images for presentation purposes. (*B*) Time course of bouton fluorescence increase during 30 Hz stimulation for 60 s in the presence of MG-2p. Data are from 4 animals (6 boutons). The bar indicates 30 Hz stimulation. (*C*) Representative traces of single puncta fluorescence increase during 30 Hz stimulation for 60 s. (*D*) Pseudocolor images of boutons coexpressing Dilp2-FAP (magenta) and BRP-GFP (green). (*E*) Representative images of boutons coexpressing Dilp2-FAP and a TeTx light chain before (Pre) and after (Stim) 70 Hz stimulation for 1 min in the presence of MG-2p. (*F*) Quantification of activity-dependent response in boutons expressing Dilp2-FAP in the control (Con) and boutons coexpressing Dilp2-FAP and TeTx as an increase in MG-2p activated FAP fluorescence in response to 70 Hz stimulation for 1 min. Data are from 6 animals (28 boutons) for each group. $^{****}P < 0.001$, unpaired *t* test. Quantification based on background subtracted unfiltered data. (*G*) Representative images of Dilp2-GFP expressing boutons before (Pre) and after 70 Hz stimulation for 1 min (Stim). (*H*) Representative images of boutons coexpressing Dilp2-GFP and TeTx Pre and Stim 70 Hz stimulation. (*I*) Quantification of activity-induced DCV-mediated release, measured as loss of GFP in the Con and TeTx expressing boutons. Data are from 5 Con animals and 6 TeTx animals. $^{***}P < 0.001$, unpaired *t* test. (*J*) Contrast-enhanced fluorescence images of Dilp2-FAP expressing boutons during 30 Hz stimulation for 60 s in the presence of MG-2p with Ba^{2+} instead of Ca^{2+} in HL3 saline. Outline of boutons shown by the dashed line in the first panel. Numbers on the images indicate stimulation time in seconds. Data are representative of results from 3 animals (Scale bars, 2 μm in all images.)

The spontaneous opening of DCV fusion pores is surprising in light of the previously thought obligatory association of neuropeptide release with repetitive activity. However, this activity dependence might be bypassed if different mechanisms mediate activity dependent and spontaneous fusion pore opening at synapses. For SSVs, spontaneous and activity-evoked events are distinguished by the utilization of different SNARE proteins (18). For example, in *Drosophila*, spontaneous SSV-mediated release, unlike Ca^{2+}-evoked SSV-mediated transmission, persists after expression of a TeTx light chain (11) and in nSyb null mutants (12). Likewise, spontaneous synaptic DCV fusion pore formation at the NMJ persisted with TeTx light chain expression (TeTx, Fig. 5 *A* and *B*) even though activity-evoked events were inhibited (Fig. 2 *E* and *F*). Thus, nSyb is not required for spontaneous release from either SSVs or

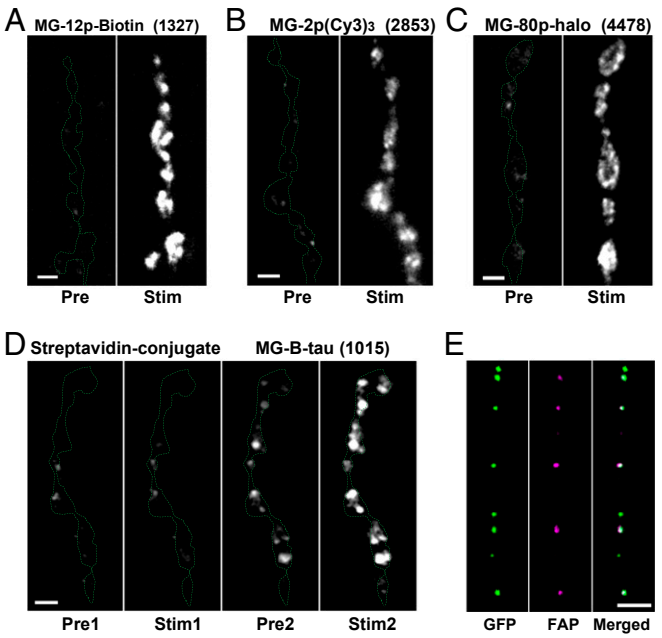

Fig. 3. FAP labeling is mediated by fusion pores. Representative images of Dilp2-FAP expressing boutons before (Pre) and after 70 Hz stimulation for 1 min (Stim) in the presence of MG-12p-biotin (*A*), MG-(Cy3)3 (*B*), and MG-p80 (*C*). Boutons outlined with the dashed line. Numbers in parentheses are MW in daltons of the MG derivative. (*D*) Representative mages of Dilp2-FAP expressing boutons in the presence of MG-12p-biotin conjugated with streptavid before (Pre1) and after 70 Hz stimulation for 1 min (Stim1) and after replacing the conjugate with MG-B-tau (Pre2) and after 70 Hz stimulation for 1 min (Stim2). (*E*) Pseudocolor images of DCVs in the axon coexpressing Dilp2-FAP (magenta) and Dilp2-GFP (green) fixed in paraformaldehyde 5 min after 70 Hz stimulation for 60 s in the presence of MG-2p (Scale bars, 2 μm.)

DCVs, although this SNARE is required for activity-dependent release from both vesicle types. The SNAP-25 G50E mutant that increases spontaneous SSV "minis" (19) also increased spontaneous DCV fusion pore opening frequency (Fig. 5*B*). Thus, spontaneous release by SSVs and DCVs depend similarly on SNARE proteins, suggesting a conserved mechanism for spontaneous release from the two vesicle classes.

Finally, we targeted Syx1A, whose H_{abc} domain selectively regulates spontaneous SSV fusion events without being required for evoked SSV-mediated release (20). Specifically, because knockout of Syx1A is lethal, a Syx1A RNAi was expressed in type Is motor neurons that resulted in moderate knockdown of Syx1A expression (*SI Appendix*, Fig. S2). Strikingly, spontaneous DCV fusion pore opening frequency was reduced dramatically either in the absence or in the presence of extracellular Ca^{2+} (Fig. 5 *B* and *C*), but activity-dependent Dilp2-FAP responses were unaffected (Fig. 5*D*). This differential effect, complementary to the differential effect of the TeTx light chain, shows that spontaneous DCV fusion pore openings are not simply low frequency versions of activity-dependent Ca^{2+}-evoked events. Rather, activity-evoked and spontaneous opening of neuropeptide-conductive synaptic fusion pores differ mechanistically.

Optical studies of single fusion pores have been conducted on nonneuronal granules with methodology that is optimal in vitro (e.g., total internal reflection fluorescence and stimulated emission depletion), but FAP imaging can resolve initial fusion pore opening and permeation properties at an intact native synapse. FAP-MG signals showed that synaptic DCV fusion pore conduction is sufficient for transmission by the ∼90% of *Drosophila* neuropeptides, which are <4.5 kDa. Future development of larger MG derivatives will enable monitoring of synaptic fusion pores that are permeable to much larger released proteins, such the bone morphogenic protein Gbb and the neurohormone bursicon (each is ∼30 kDa). Indeed, with utilization of different spectral variants, it may be possible to directly monitor fusion pore opening and expansion that distinguishes the release of cargos of varying sizes and chemical properties.

FAP imaging also revealed a distinct mode of spontaneous synaptic DCV fusion pore opening that differs in SNARE dependence and occurs in the absence of Ca^{2+} influx. Remarkably, although DCVs do not utilize active zones, this spontaneous release appears mechanistically similar to spontaneous small molecule transmitter release by SSVs. This implies that, in the absence of activity, there is still neuropeptide release to provide a peptidergic synaptic tone, similar to the functionally important synaptic tone mediated by spontaneous SSV-mediated release (18, 21, 22). For example, the resultant baseline signaling could be the subject

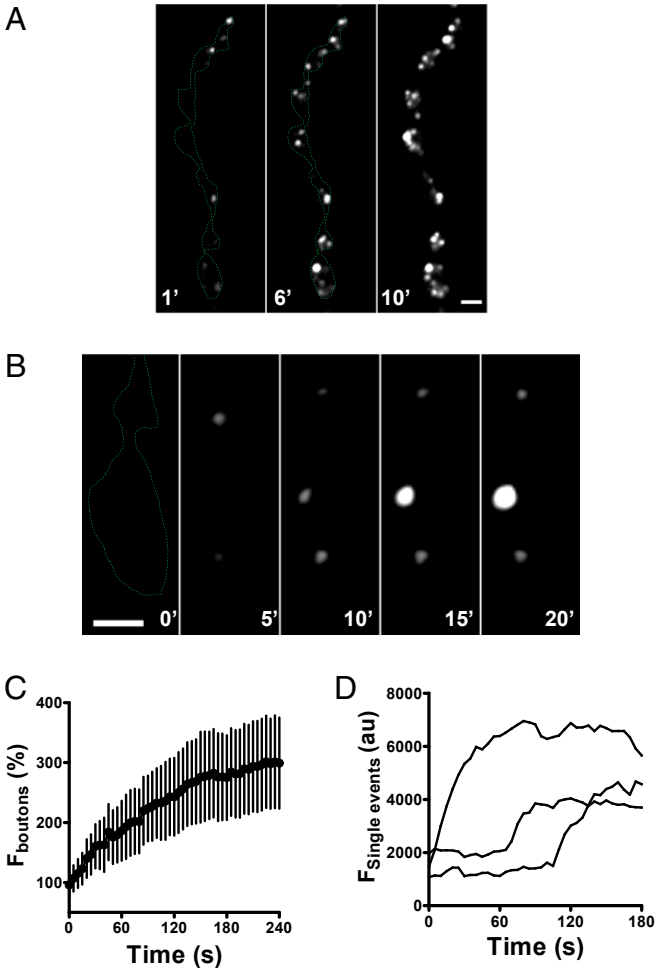

Fig. 4. Spontaneous fusion pore openings in Dilp2-FAP expressing boutons in the presence of MG-2p. (*A*) Representative images of Dilp2-FAP expressing boutons in the absence of Ca^{2+} after application of MG-2p. Numbers on the images indicate minutes. (*B*) Consecutive images of Dilp2-FAP expressing boutons in the absence of Ca^{2+}after application of MG-2p show that individual puncta vary in whether they grow brighter with time. Numbers on the images indicate minutes (Scale bars, 2 μm.) (*C*) Time course of bouton fluorescence increase in the absence of Ca^{2+} after application of MG-2p. Data are from 5 animals (12 boutons). (*D*) Representative time courses of individual spontaneous fusion pore openings in the absence of Ca^{2+} after application of MG-2p.

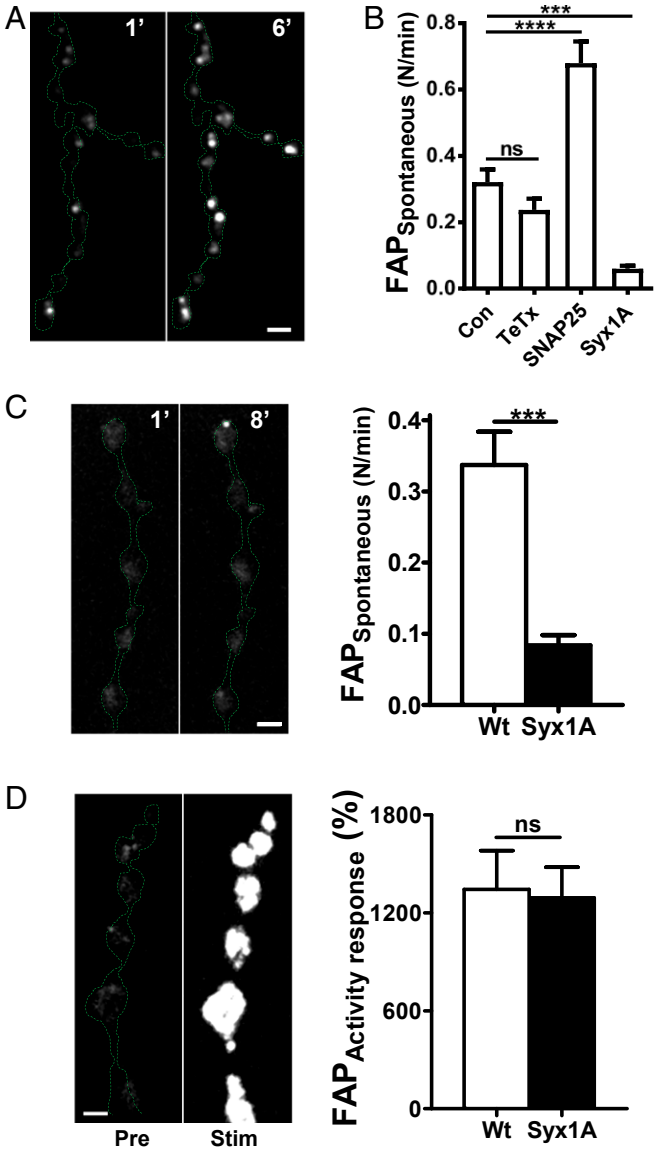

Fig. 5. SNARE dependence of spontaneous fusion pore opening. (*A*) Representative images of boutons coexpressing Dilp2-FAP and TeTx in the absence of Ca^{2+} after application of MG-2p. Numbers on the images indicate time in minutes. Note spontaneous brightening of the FAP signal. (*B*) Frequency of spontaneous fusion pore openings in the absence of Ca^{2+} analyzed as a number of fusion pore openings per bouton per minute. Data are from 6 animals for Con, (59 boutons), 4 animals for TeTx expressing boutons (19 boutons), 6 animals for SNAP25 G50E mutant (35 boutons), 7 animals for syntaxin 1A (Syx1A) RNAi expressing boutons (115 boutons). ***$P < 0.001$, ****$P < 0.0001$, Dunnett's posttest following one-way ANOVA ($P < 0.0001$). (*C*, *Left*) Representative images of boutons coexpressing Dilp2-FAP and Syx1A RNAi after application to MG-2p in the presence of Ca^{2+}. Numbers on the images represent minutes. (*Right*) Frequency of spontaneous fusion pore openings in normal Ca^{2+} saline. Data are from 4 animals in wild type (WT) animals (38 boutons) and 4 animals for Syx1A RNAi expressing boutons (43 boutons). ***$P < 0.001$, unpaired *t* test. (*D*, *Left*) Representative images of boutons coexpressing Dilp2-FAP and Syx1A RNAi Pre and Stim 70 Hz stimulation for 1 min. (*Right*) Quantification of Dilp2-FAP response in WT and Syx1A RNAi expressing boutons. Data are from 6 animals for WT (28 boutons) and 5 animals for Syx1A RNAi expressing boutons (28 boutons) (Scale bars, 2 μm.)

of regulation by opposing signaling pathways (e.g., G_s- versus G_i-coupled receptors). More generally, spontaneous opening of neuropeptide permeable fusion pores at synapses provides background neuromodulation upon which activity-dependent transmission operates. By controlling spontaneous and activity-evoked release of neuronal DCV cargos, synaptic DCV fusion pores govern peptidergic neurotransmission.

Methods

Flies. A synthetic DNA construct containing a fusion of rat preproANF with a myc epitope tag and FAP dimer sequence dL5** (8) was synthesized by GenScript. Using that DNA as a template, PCR was performed using primers 5′-AGC AGC AGC AGA ACA AAA ACT CAT CTC AGA AGA GGA T-3′ and 5′-CCT CCT GCG GAC AGA ACC GTC AGT TGT GTT CCA CC-3′ (IDT) and Q5 DNA polymerase for 25 cycles using manufacturer recommended conditions. The PCR product was gel purified (Invitrogen), treated with T4 polynucleotide kinase in ligation buffer, heat inactivated, then added to purified EcoRV cut and calf intestinal phosphatase treated pcDNA3-Dilp2, ligated with T4 DNA ligase, and transformed. A clone containing an in-frame insertion of the L5** FAP (8) in the C peptide of Dilp2 was selected. The clone was digested with EcoRI and XbaI and ligated into pUAS-C5 attB. All enzymes were purchased from New England Biolabs. The plasmid was injected and inserted in the VK1(2R)59D3 docking site by Genetivision. Expression was driven by recombination with ShakB-Gal4 (kindly provided by Tanja Godenschwege, Florida Atlantic University).

Upstream activator sequence (UAS)-Brp-GFP (#36292), UAS-TeTx (#28838), and Syx1A RNAi (#25811) lines were from Bloomington Stock Center. ShakB > Dilp2-GFP flies were kindly provided by John Kuwada (University of Michigan). SNAP25 G50E flies were provided by David Deitcher (Cornell University).

Imaging. MG derivatives were synthesized as previously described (7, 8, 10, 14). Streptavidin (Pierce, Thermofisher) was mixed with MG-12p-biotin in a 1:2 stoichiometry and then spun through a Biogel P6 column to isolate the conjugate.

Imaging experiments were performed at type Is synaptic boutons at muscle 13 of third instar *Drosophila melanogaster* larvae. Animals were filleted in Ca^{2+} free HL3 saline supplemented with 0.5 mM EGTA. For electrical stimulation experiments they were transferred to HL3 saline which contained (in mM) 70 mM NaCl, 5 KCl, 1.5 $CaCl_2$, 20 $MgCl_2$, 10 $NaHCO_3$, 5 trehalose, 115 sucrose, and 5 sodium Hepes, pH 7.2 supplemented with 10 mM L-glutamate to prevent muscle contractions. Nerve terminals were stimulated via segmental nerves with a suction electrode (23). Data were acquired with a wide-field Olympus microscope equipped with a Yokogawa Spinning disk confocal module and a Hamamatsu electron multiplying CCD camera with a 60× 1.1 NA water immersion objective and a multipass dichroic mirror. The MG-FAP signal in living preparations was excited at 640 nm and acquired with an ET 700/75 emission filter. A 488 nm laser and standard FITC optics were used for imaging GFP. For colocalization of MG-FAP and GFP fluorescence in the axon, the preparation was fixed in 4% paraformaldehyde and imaged with 488 nm excitation and normal emission wavelengths, thus exploiting the secondary excitation peak of the MG-FAP complex. Quantification of fluorescence intensity was performed with ImageJ software (https://imagej.nih.gov/ij/) as previously described (24). Spontaneous fusion events were counted manually from time-lapse images taken for 5 min at 0.2 Hz. Statistical analysis and graphing were performed with Graphpad Prism software. Error bars represent SEM. Statistical comparison for two experimental groups was based on Student's *t* test. For multiple comparisons to a single control, one-way ANOVA was followed with Dunnett's posttest.

ACKNOWLEDGMENTS. This research was supported by NIH grants R01NS32385 (to E.S.L.), R21NS092019, and 1RF1MH114103 (to M.P.B.).

1. P. H. Taghert, M. N. Nitabach, Peptide neuromodulation in invertebrate model systems. *Neuron* **76**, 82–97 (2012).
2. M. P. Nusbaum, D. M. Blitz, E. Marder, Functional consequences of neuropeptide and small-molecule co-transmission. *Nat. Rev. Neurosci.* **18**, 389–403 (2017).
3. A. N. van den Pol, Neuropeptide transmission in brain circuits. *Neuron* **76**, 98–115 (2012).
4. A. Merighi, Costorage of high molecular weight neurotransmitters in large dense core vesicles of mammalian neurons. *Front. Cell. Neurosci.* **12**, 272 (2018).
5. W. Shin *et al*., Visualization of membrane pore in live cells reveals a dynamic-pore theory governing fusion and endocytosis. *Cell* **173**, 934–945.e12 (2018).
6. M. Y. Wong, S. L. Cavolo, E. S. Levitan, Synaptic neuropeptide release by dynamin-dependent partial release from circulating vesicles. *Mol. Biol. Cell* **26**, 2466–2474 (2015).
7. C. Szent-Gyorgyi *et al*., Fluorogen-activating single-chain antibodies for imaging cell surface proteins. *Nat. Biotechnol.* **26**, 235–240 (2008). Erratum in: *Nat. Biotechnol.* **26**, 470 (2008).
8. C. Szent-Gyorgyi *et al*., Malachite green mediates homodimerization of antibody VL domains to form a fluorescent ternary complex with singular symmetric interfaces. *J. Mol. Biol.* **425**, 4595–4613 (2013).
9. G. K. Zupanc, Peptidergic transmission: From morphological correlates to functional implications. *Micron* **27**, 35–91 (1996).
10. Q. Yan *et al*., Near-instant surface-selective fluorogenic protein quantification using sulfonated triarylmethane dyes and fluorogen activating proteins. *Org. Biomol. Chem.* **13**, 2078–2086 (2015).
11. S. T. Sweeney, K. Broadie, J. Keane, H. Niemann, C. J. O'Kane, Targeted expression of tetanus toxin light chain in Drosophila specifically eliminates synaptic transmission and causes behavioral defects. *Neuron* **14**, 341–351 (1995).
12. D. L. Deitcher *et al*., Distinct requirements for evoked and spontaneous release of neurotransmitter are revealed by mutations in the Drosophila gene neuronal-synaptobrevin. *J. Neurosci.* **18**, 2028–2039 (1998).
13. Y. Liu, Y. Sugiura, T. C. Südhof, W. Lin, Ablation of all synaptobrevin vSNAREs blocks evoked but not spontaneous neurotransmitter release at neuromuscular synapses. *J. Neurosci.* 10.1523/JNEUROSCI.0403-19.2019 (2019).
14. C. Szent-Gyorgyi, B. F. Schmidt, J. A. Fitzpatrick, M. P. Bruchez, Fluorogenic dendrons with multiple donor chromophores as bright genetically targeted and activated probes. *J. Am. Chem. Soc.* **132**, 11103–11109 (2010).
15. M. Y. Wong *et al*., Neuropeptide delivery to synapses by long-range vesicle circulation and sporadic capture. *Cell* **148**, 1029–1038 (2012).
16. M. S. Anderson, M. E. Halpern, H. Keshishian, Identification of the neuropeptide transmitter proctolin in Drosophila larvae: Characterization of muscle fiber-specific neuromuscular endings. *J. Neurosci.* **8**, 242–255 (1988).
17. C. A. Taylor *et al*., Identification of a proctolin preprohormone gene (Proct) of Drosophila melanogaster: Expression and predicted prohormone processing. *J. Neurobiol.* **58**, 379–391 (2004).
18. N. L. Chanaday, E. T. Kavalali, Presynaptic origins of distinct modes of neurotransmitter release. *Curr. Opin. Neurobiol.* **51**, 119–126 (2018).
19. S. S. Rao *et al*., Two distinct effects on neurotransmission in a temperature-sensitive SNAP-25 mutant. *EMBO J.* **20**, 6761–6771 (2001).
20. P. Zhou *et al*., Syntaxin-1 N-peptide and Habc-domain perform distinct essential functions in synaptic vesicle fusion. *EMBO J.* **32**, 159–171 (2013).
21. R. W. Cho *et al*., Phosphorylation of complexin by PKA regulates activity-dependent spontaneous neurotransmitter release and structural synaptic plasticity. *Neuron* **88**, 749–761 (2015).
22. B. J. Choi *et al*., Miniature neurotransmission regulates Drosophila synaptic structural maturation. *Neuron* **82**, 618–634 (2014).
23. D. Shakiryanova, A. Tully, R. S. Hewes, D. L. Deitcher, E. S. Levitan, Activity-dependent liberation of synaptic neuropeptide vesicles. *Nat. Neurosci.* **8**, 173–178 (2005).
24. E. S. Levitan, F. Lanni, D. Shakiryanova, In vivo imaging of vesicle motion and release at the Drosophila neuromuscular junction. *Nat. Protoc.* **2**, 1117–1125 (2007).